



THE EFFECTIVENESS ACOUSTIC CONTACT ON PIEZOELECTRIC TRANSDUCERS

Francisco J. Arnold

Universidade Estadual de Campinas, Centro Superior de Estudos Tecnológicos
P.O. Box 456 – 13484-420 – Limeira, SP, Brazil

Abstract. *The piezoelectric transducers employed in high power ultrasound are composed of piezoelectric ceramics and metallic pieces. These transducers are mechanically pre-stressed in order to avoid the ceramic fractures when it is supplied with high voltage on resonance frequency. It was observed the pre-stressing application on composed transducers yields shiftings on resonance and anti-resonance characteristics. Similar effects were obtained from electric impedance curve of transducers simulations where the pieces contact transversal section was varied. These features reveal that the pre-stressing contributes for the improvement of effective acoustic contact between the transducers parts.*

Key-words: *transducers, piezoelectrics, pre-stressing, ultrasound*

1. INTRODUCTION

The high power piezoelectric transducers used in medical and industrial applications are composed of piezoelectric ceramics and mettalic pieces (backing and concentrators). Those transducers when excited by high senoidal electric voltage produce large strains that can take to ceramic fracture in the tractive semicycle. The transducers are mechanically pre-stressed up to 50 MPa to avoid the fracture, but this changes its performance.

We have found few studies about the mechanical pre-stressing on scientific literature, which, in its major part, were written in 60's and 70's (Nishi, 1966; Krueger, 1967; Meeks *et al.*, 1975; Tims, 1981). These studies are basically experimental investigations about ceramic static behaviour and they do not take into account a mathematical model to justify the obtained results.

In this paper we investigate the effects of mechanical pre-stressing (up to 50 MPa) on the resonance and anti-resonance frequency shifting of symmetric composed transducers. We have considered two main hypothesis to explain these frequencies shiftings: the variation of ceramic physical characteristic and the variations of efective contact area between prestressed transducers pieces. The first was experimentally investigated and the second was studied through of comparison between data of mathematical model simulations and experimental results.

2. THEORY

The model to be developed intends to obtain the electric impedance expression of composed transducers, because it has all coefficients found on piezoelectric equations, allows the resonance and anti-resonance frequencies identification and its measurement is easy. So, we can compare the experimental and the simulated results.

Figure 1 shows the constructive aspect of transducers used on experiments supplied by voltage source of the impedometer employed on development of experimental work (see section 3). The ceramics and the aluminium pieces are cylindrical elements with a central hole where there is a bolt that compress the assembly.

The transducers used are symmetrical, due to this, his model become simpler and we can use the schematic representation showed on Fig. 2.

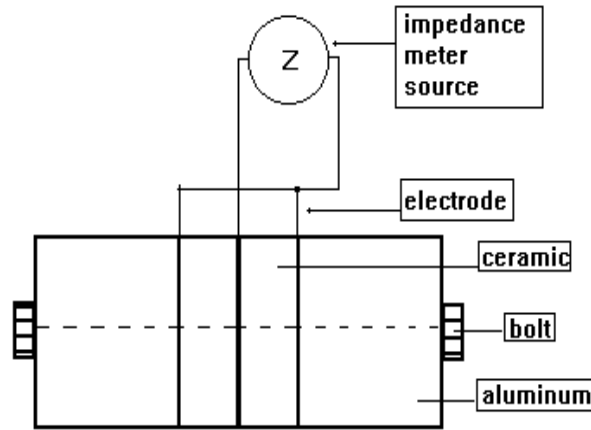


FIG. 1. Schematic representation of the transducer.

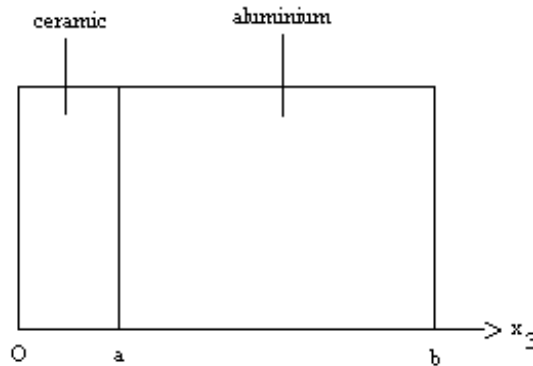


FIG. 2 Schematic representation of modeled transducer.

We have considered the following assumptions for modelling: a) the radial dimension includes many wavelengths, b) the transducer pieces are lossless; c) the transducer vibrates on longitudinal axis only (axis x_3) with longitudinal waves; d) the masses of electrodes and the bolt are negligibles.

The equations used for modelling the transducer are the following:

1) piezoelectric ceramic:

$$\rho \frac{\partial^2 u_3}{\partial t^2} = c_{33}^D \frac{\partial^2 u_3}{\partial x_3^2} \quad (1)$$

$$T_3 = c_{33}^D S_3 - h_{33} D_3 \quad (2)$$

$$E_3 = -h_{33} S_3 + \beta_{33}^S D_3 \quad (3)$$

2) aluminium pieces:

$$\rho_A \frac{\partial^2 u_{3A}}{\partial t^2} = Y_A \frac{\partial^2 u_{3A}}{\partial x_3^2} \quad (4)$$

where

the index A is the reference to aluminium medium;

ρ is the density of propagation medium;

c_{33}^D is the elastic coefficient of ceramic defined by ratio of the stress to strain on axis 3 with electric displacement zero;

Y is Young modulus;

u_3 is the displacement of particle of propagation medium on wave propagation direction;

x_3 is the wave propagation direction;

t is the time;

D_3 is the electric displacement on axis 3;

S_3 is the strain on axis 3;

T_3 is the stress on axis 3;

E_3 is the electric field on axis 3;

h_{33} is the piezoelectric coefficient;

β_{33}^S is the inverse of electric permittivity (ϵ_{33}^S) with the clamped ceramic.

The solutions of wave equation in each medium are:

1) piezoelectric ceramic

$$u_3 = A \sin(px_3) + B \cos(px_3) \quad (5)$$

$$T_3 = pc_{33}^D [A \cos(px_3) - B \sin(px_3)] - h_{33} D_3 \quad (6)$$

2) aluminium pieces

$$u_{3A} = A l \sin(qx_3) + B l \cos(qx_3) \quad (7)$$

$$T_{3A} = qY_A [A l \cos(qx_3) - B l \sin(qx_3)] \quad (8)$$

where

$$p = \omega / v_3$$

$$q = \omega / v_A$$

ω is the angular frequency;

$v_3 = (c_{33}^D / \rho)^{1/2}$ is the velocity of longitudinal wave propagation on ceramic;

$v_A=(Y_A/\rho_A)^{1/2}$ is the velocity of longitudinal wave propagation on aluminium;
 A, B, AI, BI are constants to be calculated through continuity conditions.

When a wave propagates through a multi-layer medium reflections appears due to the impedance difference between layers. The reflections are verified too when the media transversal sections are different (Frey & Kinsler, 1950). The resolution of this kind of problems consists in to solve the wave equations in each medium and to apply the continuity conditions, which in this problem are the continuities of stress and flux volum. The continuity conditions are written by:

$$u_3(0)=0 \quad (9)$$

$$S_c u_3(a)= S_{3A} u_{3A}(a) \quad (10)$$

$$T_3(a)=T_{3A}(a) \quad (11)$$

$$T_{3A}(b)=0 \quad (12)$$

where

a is the thickness of one ceramic;

b is the thickness of the half transducer;

S_c is the transversal section of the piezoelectric ceramic;

S_A is the transversal section of the aluminium pieces.

Equation (9) is consequence of symmetry of transducer, this means the central position is clamped; Eqs. (10) and (11) establish the flux volum and stress continuity on ceramic-aluminium interface and the Eq. (12) indicates the end of transducer is free.

By solving the system produced by replacement of solutions of each media on continuity condition of problem, we can obtain E_3 and D_3 of piezoelectric equations and derive the voltage V and the electric current i by

$$= \int E_3 dx \quad (13)$$

$$i = \frac{dD_3}{dt} \quad (14)$$

The electric impedance modulus ($Z=V/i$) of the transducer is given by:

$$|Z| = \frac{1}{\omega C_0} \left(1 - \frac{h_{33}^2 s_{12}}{\beta_{33}^s a} \frac{\phi_1}{pc_{33}^D s_{12} \cot(pa) \phi_1 + qY_A \phi_2} \right) \quad (15)$$

where

$\phi_1 = \cos(qa) + \sin(qa)\tan(qb)$;

$\phi_2 = \sin(qa) - \cos(qa)\tan(qb)$;

s_{12} is the ratio of transversal section (S_c/S_A).

3. EXPERIMENTAL METHOD

The experimental results were obtained with the construction of some composed transducers similars to the Fig. 1. These transducers are composed of two ring piezoelectric ceramics with 6.3 mm of thickness and 12.5 and 38.0 mm of internal and external diameter respectively, with

electrodes silvered coated on planes surfaces, produced by THORNTON-INPEC - Brazil; electrodes of brass with 0.5mm of thickness; two pieces of comercial aluminium with the radial dimensions equals to ceramics and a steel bolt that pre-stresses the system when tightened. The difference between transducers is the lenght of the aluminium pieces.

The value of the pre-stressing is obtained through the calibration curve previously made. The experimental setup employed is showed on Fig. 3. When we aply a compression on ceramics, they accumulate electric charges which can be charged by a capacitor connected on parallel, converted in voltage and measured by electronic voltmeter, so that, it is possible to obtain a relation between applied force and voltage on capacitor and to determine the piezoelectric coefficient d_{33} by ratio of the accumulated charges and applied force on ceramic. The piezoelectric coefficient h_{33} used on model is derived {Berlincourt *et al*, 1964) by

$$h_{33} = \beta_{33}^T c_{33}^D d_{33} \quad (16)$$

where

β_{33}^T is the inverse of electric permittivity of free ceramic.

The transducers are mounted and the ceramics connected to dispositives 3 and 4 of montage showed on Fig. 3. When the bolt tights the assembly, the voltmeter indicates a voltage that will be converted in stress throught previously calibration curve obtained..

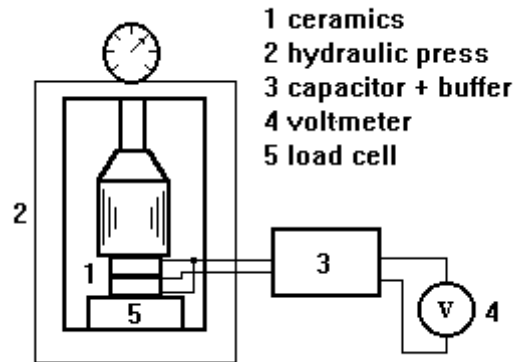


FIG. 3. Experimental set up for calibration of the compression.

After that, we disconnect the dispositives 3 and 4 and the transducer is supplied by a fasorial impedometer (HP4192A) with a senoidal excitation signal of 1.0 V. The impedometer also provides the resonance and anti-resonance frequency lectures of the system.

The values of dielectric, elastic and piezoelectric coefficients were obtained through static measures (Berlincourt *et al*, 1964; ANSI/IEEE, 1976).

The verification about the elastic coefficient shifting was done by pulse-echo method (Wells, 1977). Considering that the Young modulus of the aluminium does not vary when the material is submitted to compression up to 50 MPa and measuring the time of transit of a pulse in the transducer, we can determinate the wave velocity (v) in the transducer and derive the elastic coefficient by $c_{33}^D = \rho v^2$.

We have mounted 4 transducers called T1, T2, T3 and T4. They have aluminium pieces with 13, 26, 33 e 37mm respectively of the thickness in each end. In each transducer was

measured the resonance and anti-resonance frequencies relative to several mechanical pre-stressing..

The acoustical contact was studied through simulations. The transversal section of the ceramic was attributed equal to 1 and of the aluminium pieces on range 0.1 to 1. For the simulations, the values of the ceramic characteristics were obtained experimentally. The values of modulus de Young ($Y_A=11,1\times 10^{10}\text{N/m}^2$) and longitudinal wave propagation velocity ($v_A=6420\text{m/s}$) of aluminium pieces, respectively, were obtained from a table (Edmonds, 1981).

4. RESULTS

The results are showed in two parts: firstly we presented the results of ceramic characterization and the static measures realized with the transducer for identification of relations between physical characteristics of the ceramic and of the mechanical pre-stressing; secondly we presented graphics of resonance and anti-resonance frequencies relatives to pre-stressing and to ratio of transversal sections (s_{12}) in the transducers.

4.1 Ceramic Characterization

The ceramics characteristics were measured according to standard ANSI/IEEE (1976) and they were obtained: $\epsilon_{33}^S = 11 \text{ nF/m}$, $c_{33}^D = 13,9 \times 10^{10} \text{ N/m}^2$, $v = 4325\text{m/s}$.

The dielectric coefficient presents a little increasing proportional to applied mechanical pre-stressing, which it can be neglected. The elastic and piezoelectric coefficients did not present variations relative to pre-stressing. The piezoelectric coefficient measured was d_{33} ($d_{33} = 366\times 10^{12} \text{ C/N}$) and in the simulations was employed $h_{33} = 14,8\times 10^8 \text{ N/C}$ (Berlincourt *et al*, 1963).

4.2 Experimental and Simulations Results

Figures 4 to 7 show the graphics of resonance and anti-resonance frequencies as function of mechanical pre-stressing obtained by proposed methodology. Figures 8 to 11 show the graphics obtained of simulations performed with model described on section 2 as function of ratio of transversal sections of ceramic and aluminium piece. The superior curves represent the anti-resonance frequency and the inferior ones the resonance frequency.

5. DISCUSSION

Through results obtained with static measures we can say the mechanical pre-stressing (up to 50 MPa) does not yield remarkable changes on ceramic physical characteristics. The dielectric coefficient showed a little increasing that causes a negligible reduction on resonance frequency. The pulse-echo method showed the velocity of propagation in the transducer is not shifted with the pre-stressing and thus, the elastic coefficient also does not change. The piezoelectric coefficient do not shift either, the calibration curve shows the voltage and the stress are linearly related.

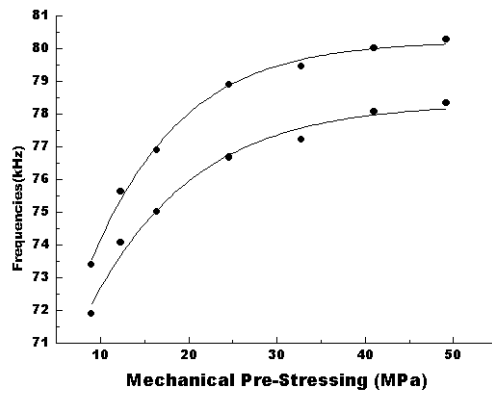


Figura 4 – Graphic of experimental results of resonance (inferior curve) and anti-resonance (superior curve) frequencies versus mechanical pre-stressing of the transducer T1 (aluminium piece thickness - 13 mm).

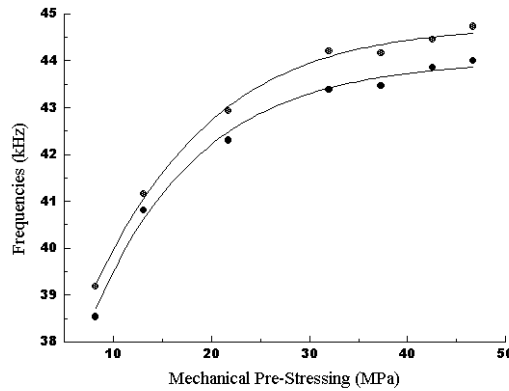


Figura 5 - Graphic of experimental results of resonance (inferior curve) and anti-resonance (superior curve) frequencies versus mechanical pre-stressing of the transducer T2 (aluminium piece thickness - 26 mm).

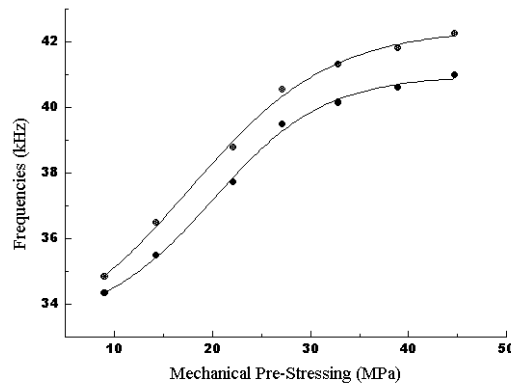


Figura 6 - Graphic of experimental results of resonance (inferior curve) and anti-resonance (superior curve) frequencies versus mechanical pre-stressing of the transducer T3 (aluminium piece thickness - 33 mm).

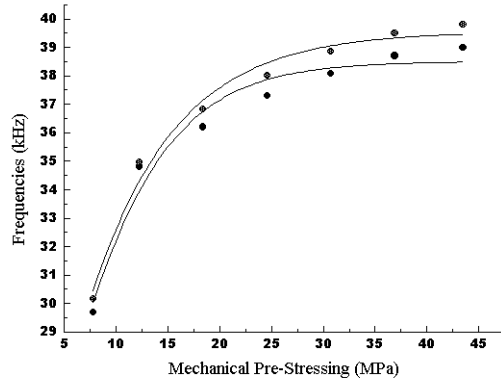


Figure 7 - Graphic of experimental results of resonance (inferior curve) and anti-resonance (superior curve) frequencies versus mechanical pre-stressing of the transducer T4 (aluminium piece thickness - 37 mm).

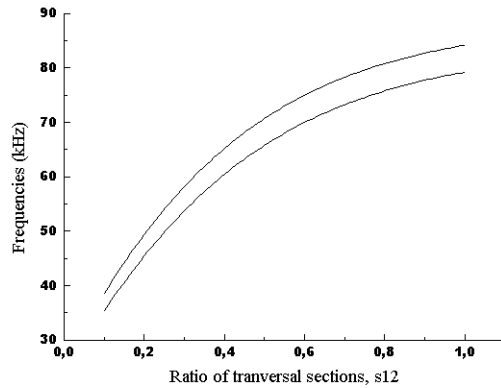


Figure 8 – Graphic of simulation results of resonance (inferior curve) and anti-resonance (superior curve) versus ratio of transversal sections (s_{12}) of the transducer T1 (aluminium piece thickness – 13 mm).

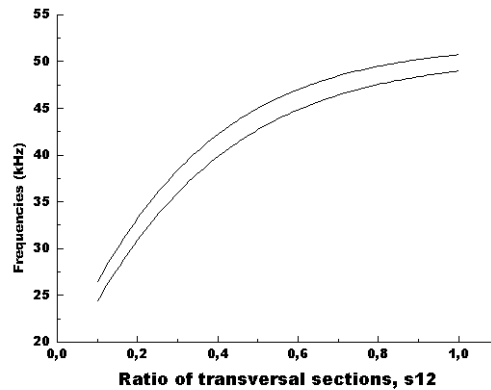


Figure 9 – Graphic of simulation results of resonance (inferior curve) and anti-resonance (superior curve) versus ratio of transversal sections (s_{12}) of the transducer T2 (aluminium piece thickness – 26 mm).

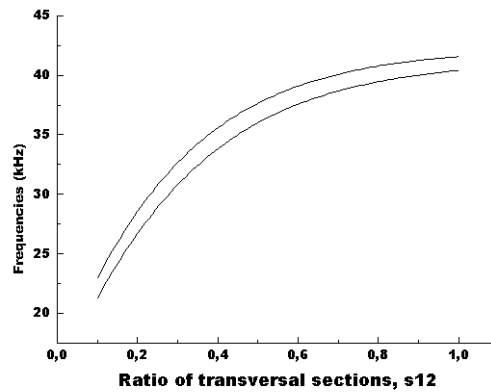


Figure 10 – Graphic of simulation results of resonance (inferior curve) and anti-resonance (superior curve) versus ratio of transversal sections (s_{12}) of the transducer T3 (aluminium piece thickness – 33 mm).

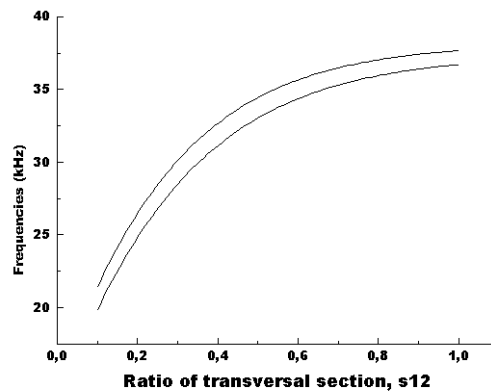


Figure 11 – Graphic of simulation results of resonance (inferior curve) and anti-resonance (superior curve) versus ratio of transversal sections (s_{12}) of the transducer T4 (aluminium piece thickness – 37 mm).

The frequencies are determined when the electric impedances modula are minimum (resonance) or maximum (anti-resonance). We have observed in the experimental results that the resonance and anti-resonance frequencies variations grow less on range of pre-stressing between 30 and 50 MPa. Similarly, in the simulation results, we can see the same tendency when the transversal section ratio is larger to 0.7. We can say that the effective acoustic contact between pieces increases proportionally to pre-stressing. Thus, the observed changes on frequencies are caused by variations on effective coupling between transducer parts. The entire contact between the pieces occurs when $s_{12}=1$, so we can say this contact approximates to ideal value when the pre-stressing is larger to 30 MPa.

In all transducers the shape of experimental and simulated curves are similar. In the transducers T1 and T2, the highest frequencies measured are smaller than ones obtained in the simulations when $s_{12}=1$ (see Figs. 4, 5, 8, 9). In the transducers T3 and T4 these experimental values are larger than ones of the simulation (see Figs. 6, 7, 10, 11). In the transducers T3 and T4 these discrepancies are caused by difference between Young modulus of aluminium used on transducer and that found in the table (Edmonds, 1981). In the transducers T1 and T2,

these differences can be caused by mechanical charge of the bolt. The mechanical charge of the transducer is the main factor to determine the resonance and the anti-resonance frequencies of the system. In these transducers the volume of aluminium is small, thus the difference between mass of aluminium and steel (bolt) decreases and the impedance average of metallic parts increases yielding decreasing on resonance frequency.

6. CONCLUSIONS

We can conclude that mechanical pre-stressing improves the acoustical contact between transducers pieces on application range up to 50 MPa and does not alter the physical parameters of ceramics and metallic pieces.

From technological point of view, we suggest that the determination of resonances of the ultrasonics transducers for application on range some tens of kHz be done with the system pre-stressed with at least 30 MPa. This guarantees a best coupling between transducer parts reducing the losses and the transducers duty frequencies can be determined approximately, using $s_{12} = 1$ in the proposed model.

7. ACKNOWLEDGEMENTS

The author is grateful to Dr. Sérgio Mühlen from CEB/UNICAMP by technical support and Dr. Rubens Sigelmann from Washington University by discussions about the subject.

8. REFERENCES

ANSI/IEEE, 1978 Standard on Piezoelectricity 176.

Berlincourt, D., Curran, D. & Jaffe, H., 1964, Piezoelectric and Piezomagnetic Materials and Their Function in Transducers, Physical Acoustics, vol.1(A), pp. 170-270.

Edmonds, P., 1981, Ultrasonics, Methods of Experimental Physics, Academic Press , New York.

Kinsler, A. & Frey, L., 1950, Fundamentals of Acoustics, John Wiley & Sons, New York.

Krueger, H., 1968, Stress Sensitivity of Piezoelectric Ceramics: Part 3. Sensitivity to Compressive Stress Perpendicular to the Polar Axis, The Journal of the Acoustical Society of America, vol.43(3), pp.583-591.

Meeks, S & Timme, R., 1975, Effects of one-dimensional stress on piezoelectric ceramics, Journal of Applied Physics, vol.46(10), pp.4334-4338.

Nishi, R., 1966, Effects of One-Dimensional Pressure on the Properties of Several Transducer Ceramics, The Journal of the Acoustical Society of America, vol.40(2), pp.486-495.

Ristic, V., 1982, Principles of Acoustic Devices, John Wiley & Sons, New York.

Tims, A., 1981, Effects of multidimensional stress on radially polarized piezoelectric ceramic tubes, The Journal of the Acoustical Society of America, vol.70(1), pp.21-28.

Wells, P. , 1977, Biomedical Ultrasonics, Academic Press, New York.